International Journal of Chemical, Materials and Biomolecular Sciences
ISSN: 2415-6620
Vol:11, No:1, 2017

Air Classification of Dust from Steel Converter Secondary De-dusting for Zinc Enrichment

C. Lanzerstorfer

***Abstract*—**The off-gas from the basic oxygen furnace (BOF), where pig iron is converted into steel, is treated in the primary ventilation system. This system is in full operation only during oxygen-blowing when the BOF converter vessel is in a vertical position. When pig iron and scrap are charged into the BOF and when slag or steel are tapped, the vessel is tilted. The generated emissions during charging and tapping cannot be captured by the primary off-gas system. To capture these emissions, a secondary ventilation system is usually installed. The emissions are captured by a canopy hood installed just above the converter mouth in tilted position. The aim of this study was to investigate the dependence of Zn and other components on the particle size of BOF secondary ventilation dust. Because of the high temperature of the BOF process it can be expected that Zn will be enriched in the fine dust fractions. If Zn is enriched in the fine fractions, classification could be applied to split the dust into two size fractions with a different content of Zn. For this air classification experiments with dust from the secondary ventilation system of a BOF were performed. The results show that Zn and Pb are highly enriched in the finest dust fraction. For Cd, Cu and Sb the enrichment is less. In contrast, the non-volatile metals Al, Fe, Mn and Ti were depleted in the fine fractions. Thus, air classification could be considered for the treatment of dust from secondary BOF off-gas cleaning.

***Keywords*—**Air classification, converter dust, recycling, zinc.

I. Introduction

IN the integrated iron and steel-making process the pig iron is converted to steel in the BOF or converter. The off-gas from the BOF is treated in the primary ventilation system. During oxygen blowing, the converter vessel is in a vertical position. Thus, the emissions from the converter are captured by the primary ventilation system. For charging of pig iron and scrap, as well as for tapping of slag and steel, the converter vessel has to be tilted. Consequently, the primary off-gas system cannot capture the emissions produced during these process steps. Therefore, a secondary ventilation system is installed. Via a canopy hood, which is usually installed just above the converter mouth, the emissions are extracted. A doghouse around the remaining three quarters of the converter helps to enclose the secondary emissions. Most of the secondary dust emissions are released during charging and tapping operations. Other smaller extraction points for secondary emissions are for example at the hot metal pre-treatment steps (re-ladling, de-slagging and desulfurization of hot metal), the secondary metallurgy and the casting. Cleaning of the secondary off-gas is usually performed by means of a bag filter although dry ESPs are also used. Estimates of the quantity of secondary dust emissions are up to 1 kg/t liquid steel [1].

The dust separated by the secondary ventilation system consists mainly of Fe (32-63%) [2]. Thus, secondary BOF dust is often recycled via the sinter plant. The total amount of Zn in the charge of a BF is usually restricted to 100–150 g/t of hot metal produced [1] and the Zn in the charge of the BF is mainly contained in the sinter [3]. As the de-zincing efficiency of the sintering process is quite low [4] the overall Zn content of the sinter plant feed material must be kept below a certain limit which is typically below 200 g/t. Therefore, residues recycled via the sinter plant are limited with respect to their Zn content. The Zn content of the BOF dust from the secondary ventilation system is in the range of 0.5 to 13% [1], [5]. Secondary BOF dust with a higher Zn content will therefore be excluded from recycling to the sinter plant. However, recycling into the converter after agglomeration of the dust can be done.

When a component is enriched in the fine fraction of a dust, classification can be applied to split the dust into two size fractions with a different concentration of this component. In dusts from metallurgical processes Zn can be enriched in the fine fractions. Air classification has been applied to treat the dust collected by the dust-catcher of a blast furnace [6] and the dust from a second stage fabric filter for de-dusting of blast furnace top-gas to separate a fine fraction with increased Zn content [7], [8]. However, there is no information available regarding the distribution of Zn in BOF secondary ventilation dust.

The aim of this study was to investigate the separation of BOF secondary ventilation dust into one fraction which is depleted in Zn and another fraction which is enriched in Zn. Laboratory air classification experiments with such a dust were performed.

II. Material and Methods

A. Sample Preparation

The dusts investigated originated from the secondary de-dusting system of two different BOF steelmaking plants. In both plants a fabric filter is used for de-dusting. Dust samples of approximately 2 dm³ were collected at the dust discharge systems of the fabric filters. The dust sample with the higher zinc content (the dust sample from plant A) was split into four size fractions by air classification. Prior to classification the dust sample was sieved using a 400 µm sieve to remove some coarse particles which appeared to be hardened wall deposits of dust. The dust fraction < 400 µm was air classified using a

C. Lanzerstorfer is with University of Applied Sciences Upper Austria, Wels, 4600 Austria (phone: +43-050804-43220; fax: +43-050804-943220; e-mail: c.lanzerstorfer@fh-wels.at).

Hosokawa Alpine laboratory air classifier 100 MZR. The speed of the classifier in the three classification runs was 21,000 rpm, 11,000 rpm and 6,000 rpm. A detailed description of such a classification procedure can be found elsewhere [8].

For the measurement of the particle size distribution and for chemical analysis the volumes of the dust samples were reduced to the volume suitable for measurements using sample dividers (Haver&Boecker HAVER RT and Quantachrome Micro Riffler).

B. Measurements

The moisture content of the dust samples was measured gravimetrically using a Sartorius MA35M infrared moisture analyzer. The particle size distribution of the dust samples was measured using a Sympatec HELOS/RODOS laser diffraction instrument with dry sample dispersion.

For the determination of the concentration of metals in the dust the solid samples were dissolved by aqua regia digestion prior to analysis. The metals were measured by inductively-coupled plasma optical emission spectroscopy (Horiba Jobin Yvon Ultima 2 system). Each sample was analyzed twice. In the results the average values are presented. The average relative standard deviation calculated from the two measurements was 5.4%. The concentration of alkali metals, earth alkali metals and sulfate was analyzed by ion chromatography (Dionex ICS-1000). Details of the analytical methods can be found elsewhere [9].

Microscopic images of dust particles were taken with a scanning electron microscope TESCAN, type VEGA LM. Further information about the chemical composition of the particles was obtained by energy dispersive X-ray spectroscopy (SEM-EDX).

C. Recycling Calculations

With the results of the chemical analysis of the various size fractions, the effect of air classification on the distribution of certain elements between the coarse fraction and the fine fraction was calculated. The diagrams produced show the dependence of the fraction of a component discharged with the fines on the total fraction of fines discharged. The calculation procedure is described elsewhere in the literature [10].

III. Results

A. Converter Secondary Dust Samples

The results of the chemical analysis of the two dust samples are summarized in Table I. Dust sample A was somewhat coarser (mass median diameter: 13 µm) compared to dust sample B (mass median diameter: 12 µm). The Fe content of dust sample B was substantially higher compared to dust sample A. In contrast, the concentration of Zn in dust A was significantly higher. Also the concentrations of Al and Ca were markedly higher in dust A, while the sulfate content was lower. The concentrations of the other heavy metals and the alkali metals Na and K were very similar in both dust samples.

TABLE I
COMPOSITION OF THE DUSTS

	Dust sample A	Dust sample B
Fe	215,000	303,000
Al	6,800	1,800
Mn	15,700	16,200
Pb	6,900	6,100
Zn	144,000	27,000
Na	2,500	2,700
K	3,100	2,700
Mg	9,000	7,300
Ca	45,000	27,000
SO_4^{2-}	1,400	11,700
As	52	28
Cd	322	720
Cr	222	132
Cu	320	176
Ni	68	93
Sb	97	28
Ti	688	636
V	66	309

Concentrations in mg/kg dry dust

B. Air Classification of Converter Secondary Dust

The dust with the higher Zn content (dust A) was selected for the classification experiment. The mass median diameter of the first, second, third and fourth particle size fraction of the dust was 1.02 µm, 3.0 µm, 6.7 µm and 41 µm, respectively. Fig. 1 shows the particle size distributions of the size fractions and of the original sample of dust A. The mass fractions x_m of the four size fractions produced and their compositions are summarized in Table II. More than half of the mass of the dust was found in the coarsest size fraction 4. The majority of the finer dust - approximately 40% - was distributed evenly between the two finest size fractions, while only 4% of the dust was found in size fraction 3.

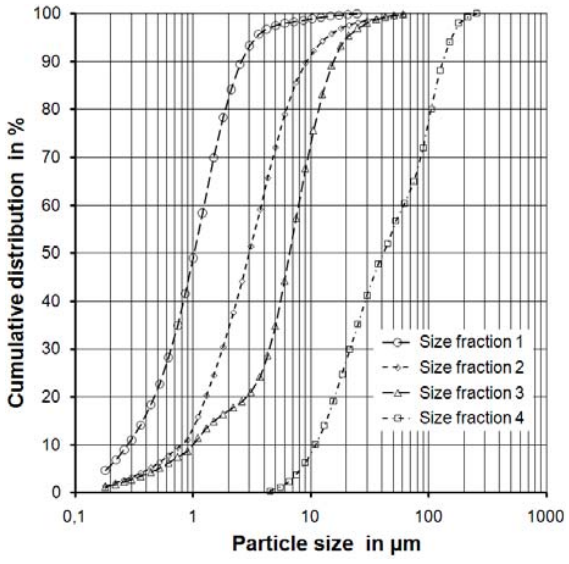

Fig. 1 Particle size distribution of the four size fractions

Microscopic images of the particles of the four size

fractions are shown in Fig. 2. The images show that there are particles of different shapes. Some particles are nearly spheres, suggesting that the material was a liquid drop that froze when the off-gas cooled down. Other particles show various shapes with edges.

On many particles a deposition of small sub-micron particles can be observed (Fig. 3). These deposits are assumed to result from material that was volatized in the converter and condensed on existing particles during cooling of the off-gas. However, the occurrence of these deposits is not equally distributed on all particles. This might be explained by the fact that the converter process is a batch process. Most of the emissions from the converter extracted by the secondary de-dusting system originate from the charging of the converter and from the tapping. Emission of volatile elements is to be expected during charging of the converter, especially when elements such as Zn are present in the scrap. In contrast, when tapping of the steel and the slag is started the volatile elements should already be discharged from the converter with the off-gas. Thus, dust particles generated during charging of the converter are more likely to show deposits of condensed matter compared to dust particles generated during tapping.

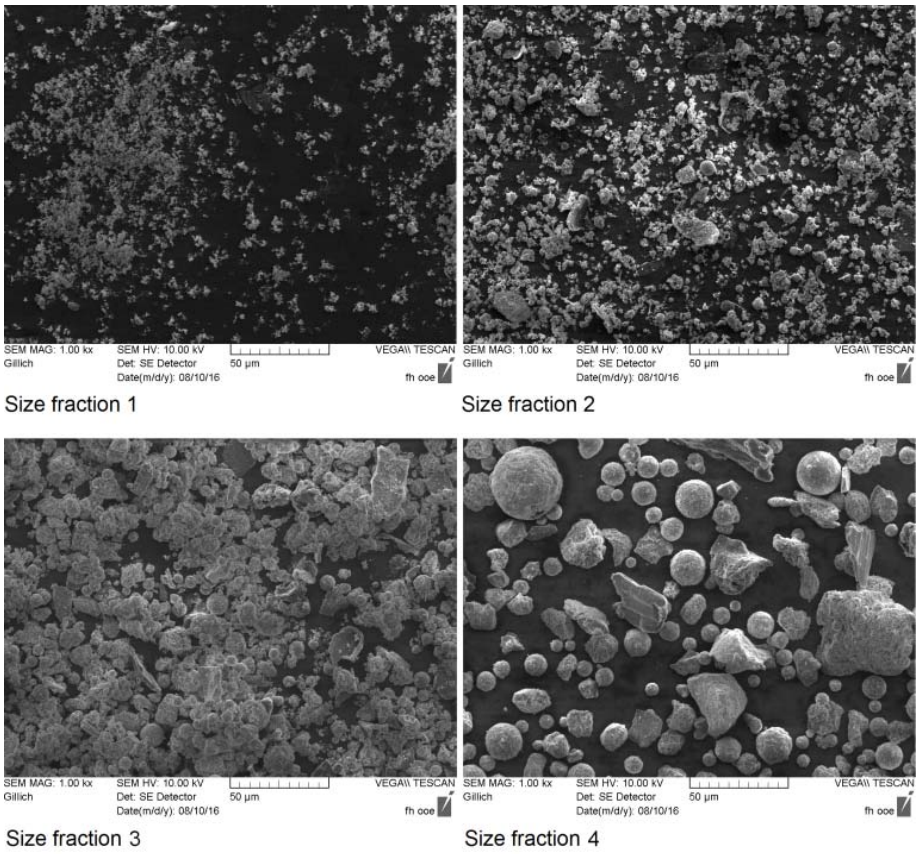

Fig. 2 Microscopic images of particles of the four size fractions

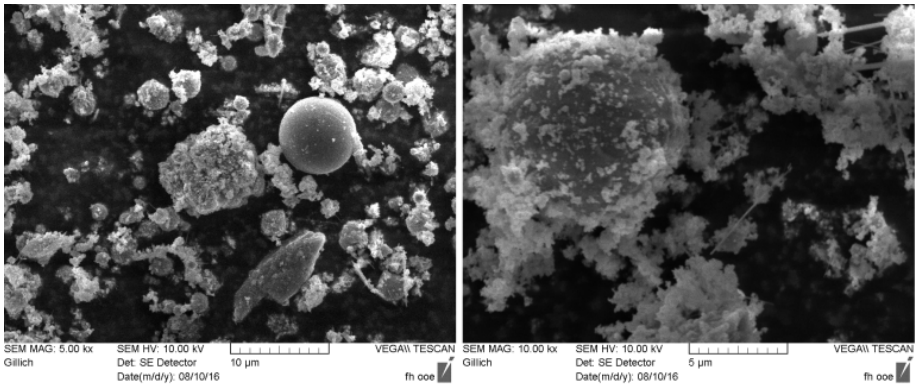

Fig. 3 Microscopic images of particles from size fraction 2

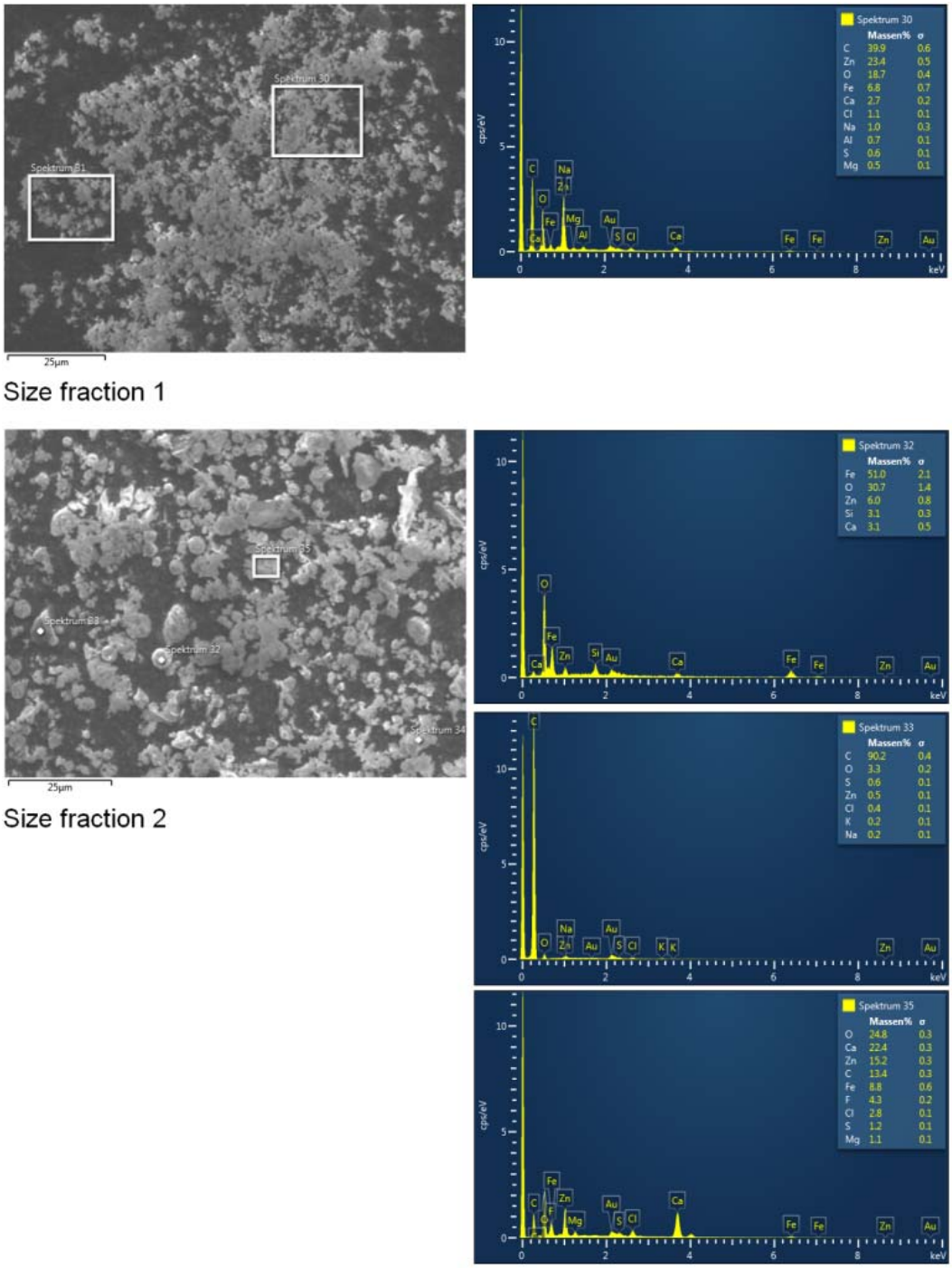

Fig. 4 EDX spectra of particles from size fraction 1 and 2

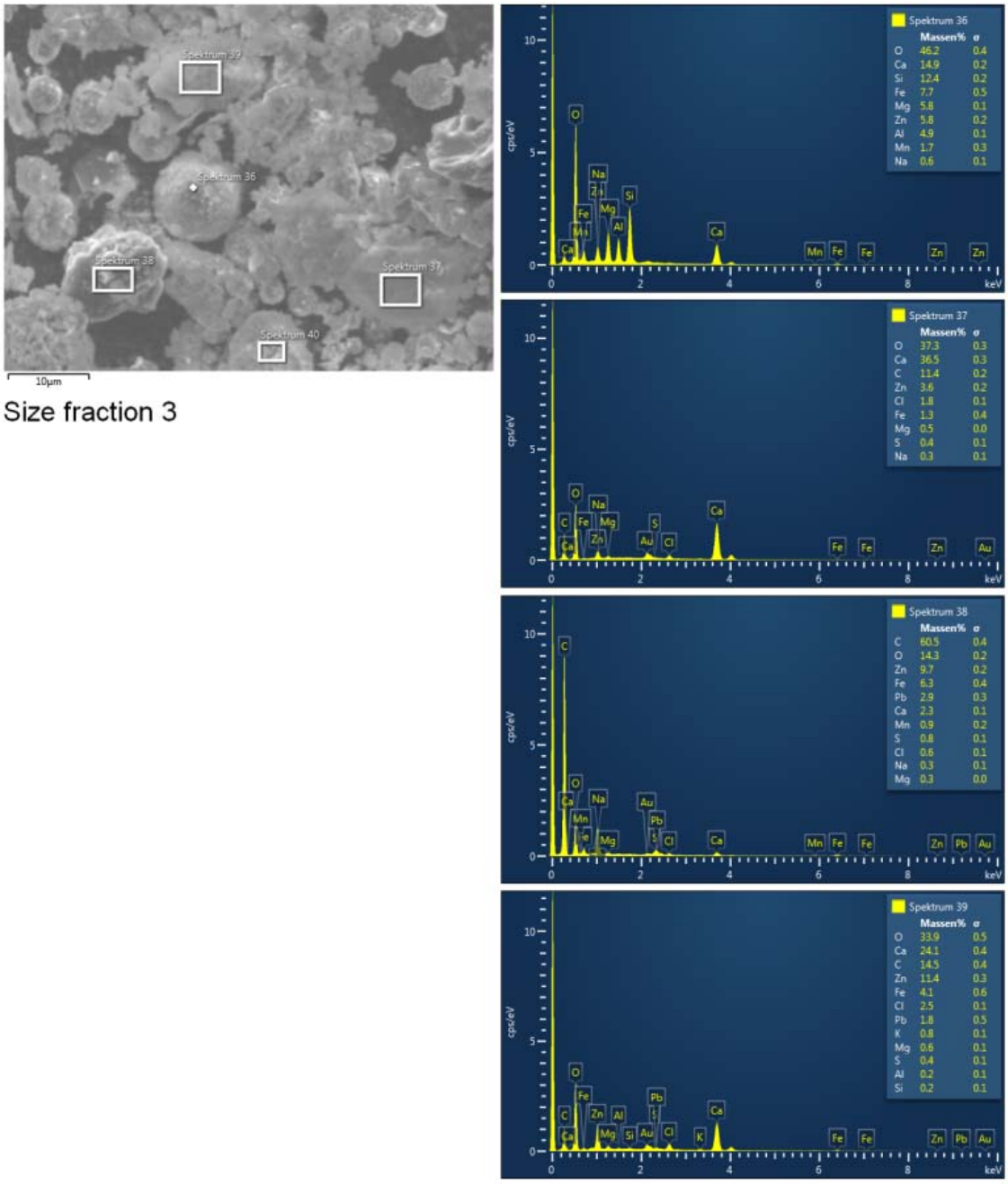

Fig. 5 EDX spectra of particles from size fraction 3

The more volatile elements Cd, Cu, Pb, Sb and Zn were enriched in the finer particle size fractions. For Cd, Cu and Sb the concentrations in size fraction 1 were roughly double the concentrations of these elements in size fraction 4. For Pb and Zn the respective enrichment was 7 times and 5 times. The enrichment of the volatile elements results from the re-condensation of these elements when the off-gas cools down in the off-gas system. The particles formed are comparatively small and, therefore they are found in the finest particle fractions. Part of the material condenses on the surface of existing particles, which also supports the enrichment because of the higher specific surface area of fine particles. In contrast, the elements Al, Fe, Ti and V were enriched in the coarser size fractions. The depletion of these elements can be explained at least partly by the dilution effect caused by the condensing material.

For As and Mn the concentrations varied with the particle size. However, no distinct size dependence was found.

The recovery rate in the classification procedure was calculated for each element. The values were in the range of

0.94 to 1.12 (Table II). In the size fractions produced the content of Cr and Ni is increased because of some erosion of material of the classifier wheel. This sample contamination has also been described in the literature [11]. Therefore, the distribution of these elements cannot be studied.

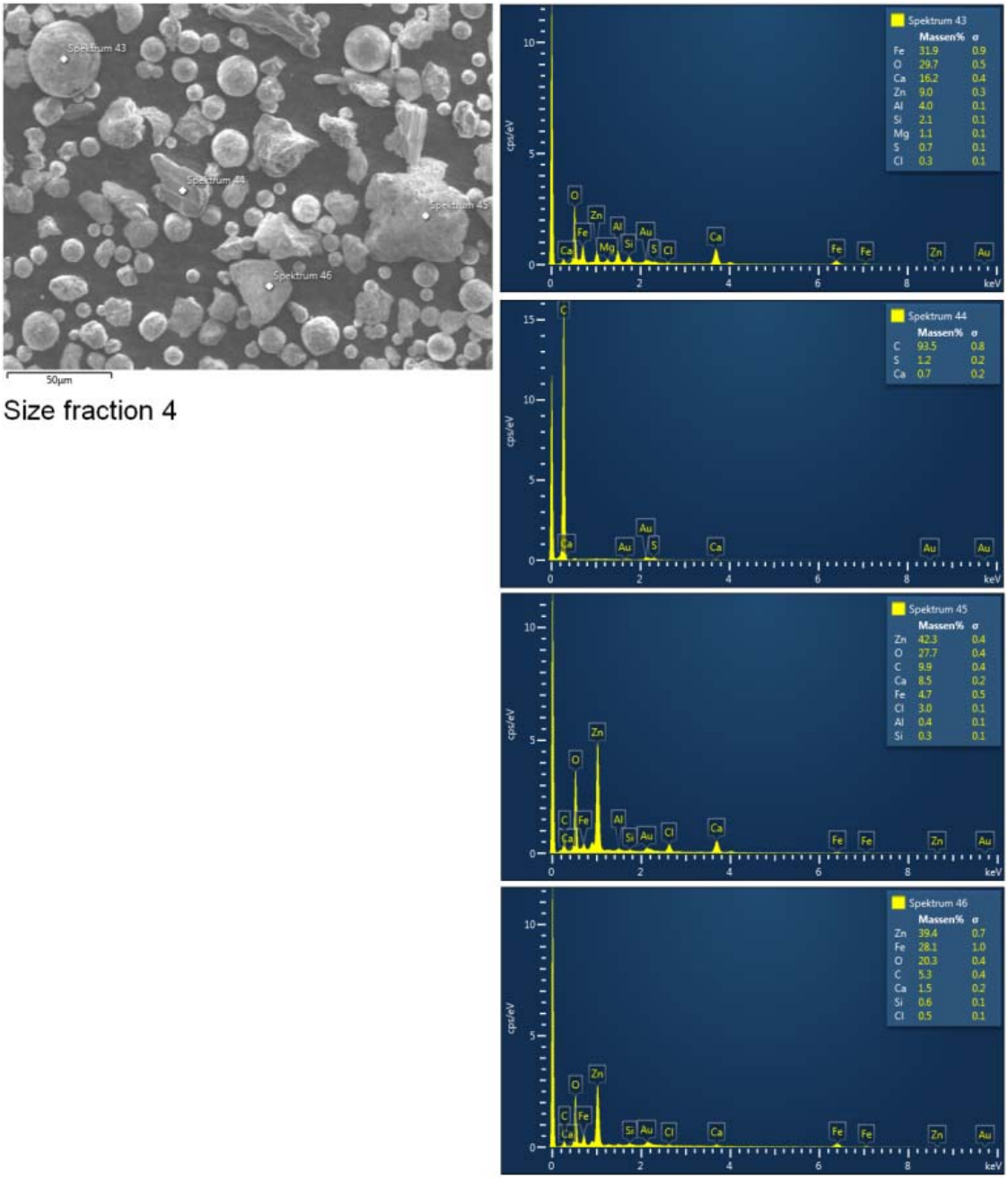

Fig. 6 EDX spectra of particles from size fraction 4

Fig. 4 shows EDX spectra of particles from size fractions 1 and 2. The spectrum of the particles from size fraction 1 (Spectrum 30) shows a high content of Zn and O. The C content is most likely an artifact from the sample-holder used, which was a double-sided adhesive tape made of carbon fiber. Spectrum 31 was quite similar but with a higher C content resulting from the larger visible area of sample-holder.

For size fraction 2 the EDX spectra of particles of various shapes are shown. Spectrum 32 is from a nearly spherical particle. It consists mainly of Fe and O, while some Zn was also detected. The shape of the particle and its composition lead to the assumption that it originates from liquid steel, which was subsequently oxidized at the surface. The irregular particle investigated by spectrum 33 consists of more than

90% C. In the agglomerate investigated by spectrum 35, besides the main components Ca, O and Zn, several other components were also detected.

TABLE II
COMPOSITION OF THE SIZE FRACTIONS OF DUST A

	Size fraction 1	Size fraction 2	Size fraction 3	Size fraction 4	Recovery
x_m	0.202	0.214	0.040	0.544	-
Al	1,930	4,180	4,960	9,430	1.00
Fe	125,000	184,000	220,000	272,000	1.03
Mn	15,030	13,000	12,900	18,500	0.97
Ti	145	516	741	896	0.95
As	53	41	35	51	0.94
Cd	559	436	275	263	1.12
Cu	415	334	284	285	1.01
Pb	16,000	12,800	6,880	2,260	1.09
Sb	151	93	61	66	0,91
V	24	43	59	88	0.98
Zn	330,000	196,000	129,000	72,300	1.06

Concentrations in mg/kg dry dust

The EDX spectra of particles from the size fractions 3 and 4 are shown in Figs. 5 and 6, respectively. The investigated spherical particle of size fraction 3 (spectrum 36) consists of Ca, Fe, Si, Mg, Al and O, which suggests it came from liquid slag. The particles investigated by spectra 37 and 39 consist mainly of O, Ca and C. The relative mass ratios of these components in the particles are nearly those of limestone. Thus, these particles are probably basically limestone particles with some other elements (Zn, Pb, Fe, K, Na, Cl, S) deposited on their surface. In the next particle (spectrum 38) C is the main component, accounting for approximately 60%. Several volatile elements can be found which might be deposited on the original particle.

The particles of size fraction 4 are comparatively large. Therefore, the spectra represent only a small amount of the surface of the particles. Thus, determination of their origin based on the spectrum measured for one point of the surface is impossible. Nevertheless, the particle investigated by spectrum 44 consists almost entirely of C, which makes it likely to be a particle of coke or carbon.

C. Recycling calculations

For the discharge of Zn from the steelmaking process, dust with a high Zn content is usually excluded from recycling. It might be sent to landfill or to a secondary Zn producer. In both cases the amount of dust which has to be discharged should be minimized. Thus, the Zn content of the discharged dust should be as high as possible.

Based on the identified dependence of the concentration of Zn and other components on the particle size of the dust size fractions a calculation of the achievable removal of Zn, Pb and Cd by air classification was performed. Fig. 7 shows the recovery of the mass of coarse dust for recycling versus the removal of specific components from the recycling with the fine dust. The curves obtained for the three volatile elements are quite similar.

If, for example, 50% of the mass of Zn contained in the dust should be removed by air classification, the fraction of the coarse dust for recycling would be approximately 70%.

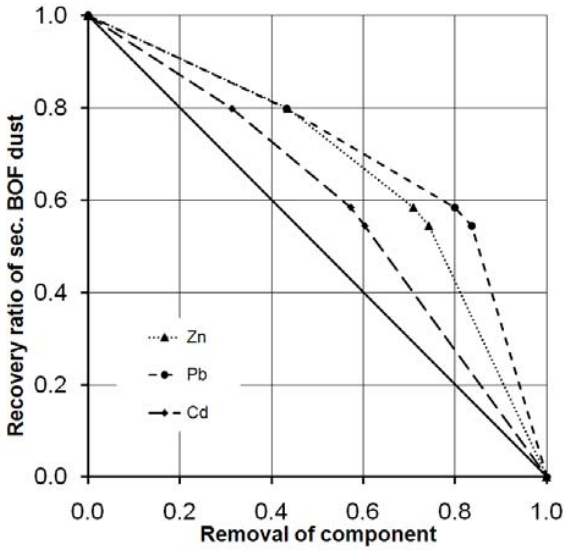

Fig. 7 Recovery of dust versus removal of specific heavy metals

Fig. 8 shows the calculated curves for Fe and Mn. These elements are depleted in the fine fraction. Therefore, the calculated curves are below the neutral line connecting the points (0/1) and (1/0). In the discussed example with a recycling rate of approximately 70% of coarse dust, the loss of Fe with the discharged fine fraction would only be approximately 15%.

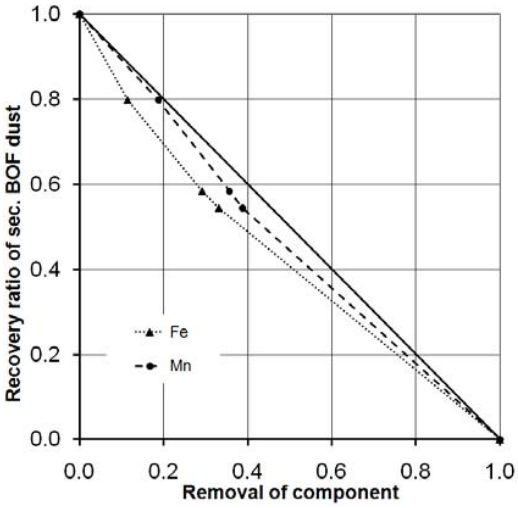

Fig. 8 Recovery of dust versus removal of Fe and Mn

ACKNOWLEDGMENT

Proofreading by P. Orgill, preparation of scanning electron microscope images by M. Gillich and laboratory work by M. Repolusk are kindly acknowledged.

REFERENCES

[1] R. Remus, M. A. Aguado-Monsonet, S. Roudier, and L. D. Sancho, "Best Available Techniques (BAT) Reference Document for Iron and Steel Production, Industrial Emissions Directive 2010/75/EU, Integrated Pollution Prevention and Control," Luxembourg: Publications Office of the European Union, 2013, pp. 15–64.

[2] S. Gara, and S. Schrimpf, „Behandlung von Reststoffen und Abfällen in der Eisen- und Stahlindustrie. M-092," Vienna: Umweltbundesamt, 1998, pp. 37–41.

[3] G. M. Stepin, L. S. Mkrtchan, I. V. Dovlyadnov, and I. K. Borshchevskii, "Problems related to the presence of zinc in Russian blast-furnace smelting and ways of solving them," Metallurgist, vol. 45, no. 9–10, pp. 382–390, 2001.

[4] C. Lanzerstorfer, B. Bamberger-Straßmayr, and K. Pilz, „Recycling of blast furnace dust in the iron ore sinter process: investigation of coke breeze substitution and the influence on off-gas emissions," ISIJ Int., vol. 55, no. 4, pp. 758-764, 2015.

[5] C. P. Heijwegen, W. Kat, "Zinc-bearing Waste Products in the Iron and Steel Industry; Their Composition and Possible Hydrometallurgic Processing Methods," World Steel and Metalworking, vol. 5, no. x, pp. 26-34, 1983.

[6] C. Lanzerstorfer, "Air classification of blast furnace dust catcher dust for zinc load reduction at the sinter plant," Int. J. Environ. Sci. Technol., vol. 13, no. 1, pp. 755-760, 2016.

[7] T. Murai, A. Kometani, Y. Ono, and T. Hashimoto, "Blast Furnace Gas Dry Cleaning System and Dry Removal System of Zing in Dry Dust," The Sumitomo Search, no. 32, pp 1-7, 1986.

[8] C. Lanzerstorfer, and M. Kröppl, "Air classification of blast furnace dust collected in a fabric filter for recycling to the sinter process," Resour. Cons. Recycl., vol. 86, no. 1, pp. 132-137, 2014.

[9] C. Lanzerstorfer, "Chemical composition and physical properties of filter fly ashes from eight grate-fired biomass combustion plants," J. Environ. Sci., vol. 30, no. 1, pp. 191-197, 2015.

[10] C. Lanzerstorfer, "Air classification: Potential treatment method for optimized recycling or utilization of fine-grained air pollution control residues obtained from dry off-gas cleaning high-temperature processing systems," Waste Manage. Res., vol. 33, no. 11, pp. 1041-1044, 2015.

[11] C. Lanzerstorfer, "Investigation of the contamination of a fly ash sample during sample preparation by classification," Int. J. Environ. Sci. Technol., vol. 12, no. 4, pp. 1437-1442, 2015.